JOURNAL OF THE ROYAL SOCIETY Interface

A constitutive model for muscle properties in a soft-bodied arthropod

A Dorfmann, B.A Trimmer and W.A Woods, Jr

J. R. Soc. Interface 2007 **4**, 257-269
doi: 10.1098/rsif.2006.0163

JOURNAL OF THE ROYAL SOCIETY Interface

J. R. Soc. Interface (2007) **4**, 257–269
doi:10.1098/rsif.2006.0163
Published online 17 October 2006

A constitutive model for muscle properties in a soft-bodied arthropod

A. Dorfmann[1,*], B. A. Trimmer[2] and W. A. Woods Jr[3]

[1]*Department of Civil and Environmental Engineering and the Biomimetic Devices Laboratory,* [2]*Department of Biology and the Biomimetic Devices Laboratory, and* [3]*Department of Biology, Tufts University, Medford, MA 02155, USA*

In this paper, we examine the mechanical properties of muscles in a soft-bodied arthropod under both passive and stimulated conditions. In particular, we examine the ventral interior lateral muscle of the tobacco hornworm caterpillar, *Manduca sexta*, and show that its response is qualitatively similar to the behaviour of particle-reinforced rubber. Both materials are capable of large nonlinear elastic deformations, show a hysteretic behaviour and display stress softening during the first few cycles of repeated loading. The *Manduca* muscle can therefore be considered as different elastic materials during loading and unloading and is best described using the theory of pseudo-elasticity. We summarize the basic equations for transversely isotropic pseudo-elastic materials, first for general deformations and then for the appropriate uniaxial specialization. The constitutive relation proposed is in good agreement with the experimental data for both the passive and the stimulated conditions.

Keywords: *Manduca sexta*; caterpillar muscles; striated muscles; tetanic stimulus; anisotropy; constitutive modelling

1. INTRODUCTION

In addition to their well-known function as biological motors, muscles also act as brakes, struts, beams and springs (Biewener 2003). For most animals with stiff skeletons, these different muscle functions are transmitted through tendon attachments to the movements of jointed levers. However, for animals that lack rigid skeletons (e.g. worms, caterpillars and molluscs), muscles are more directly coupled to overt movements and the material properties of soft tissues play a more central role in soft-bodied locomotion (Trueman 1975). Any attempt to understand how such animals control their movements must take into account the fundamental material properties of the muscles. In the study presented here, we examine the muscles of the tobacco hornworm caterpillar, *Manduca sexta*, and show that in a steady state (passive or stimulated), these muscles behave as elastomeric materials. A constitutive model is developed that describes the pseudo-elastic responses of a specific muscle and compares it with particle-reinforced natural rubber.

Manduca is commonly used in physiological studies and has recently served as a biological model for a new class of soft-bodied robots (Trimmer *et al.* 2006). The muscles, *ca* 70 per larval segment, are layered beneath the soft cuticle to which they are attached. Most lie entirely within a single segment and are innervated by a single motor neuron (e.g. Levine & Truman 1985). These muscles are tasked to function quite differently from skeletal locomotory muscles such as those in adult insects, which typically contract rapidly while undergoing limited shortening. For example, the wing muscles of adult *Manduca* cycle through a strain of *ca* 7% during flight, shortening in *ca* 0.018 s (Stevenson & Josephson 1990). In contrast, in crawling *Manduca* caterpillars, some muscles cycle through strain ranges of *ca* 30% and take a full second to shorten during a typical crawling cycle (Woods *et al.* submitted). Considerably higher strain ranges are probably encountered during other natural motions (Brackenbury 1997). The muscles can develop force *in vitro* over a strain range from 0.5 to 1.5 times their resting length. Compared with typical striated skeletal muscle, caterpillar muscles can be described as slow and stretchy.

Underlying these functional differences are differences in muscle structure. Vertebrate skeletal muscles, the most widely studied locomotory muscle type, are organized into short, distinct sarcomeres, with 6–8 thin myofilaments associated with each thick filament and very distinct aligned Z-bands. In contrast, caterpillar muscles show less organization with long sarcomeres, unevenly aligned and less distinct Z-bands, and 10–12 thin myofilaments surrounding each thick filament (Rheuben & Kammer 1980). In addition, skeletal muscle is attached to bone by tendons, which make the major contribution to the elastic properties of the muscle-tendon system (Biewener & Roberts 2000). Caterpillar muscle, in contrast, lacks associated discrete tendons. Any capacity for elastic energy storage therefore arises from properties of both the muscle

*Author for correspondence (luis.dorfmann@tufts.edu).

Received 11 July 2006
Accepted 9 September 2006

contractile elements and the extracellular tissues including collagen.

Since soft-bodied animals change shape, the passive properties of their muscles are particularly important. In common with vertebrates, invertebrate striated muscle contains elastic proteins that affect contraction and stretching (Ziegler 1994). The best characterized of these molecules is the giant protein, I-connectin, found in the muscles of barnacles, beetles, flies (both larvae and adults) and crayfish, where it appears to determine passive elasticity. This protein contains elastic domains that produce transient tension changes with complex time-constant decay (Fukuzawa *et al.* 2001). A search of the recently released silkmoth *Bombyx mori* genome by Shimada *et al.* (2004) shows that titin- and kettin-like proteins are probably present in the Lepidoptera. The elastic properties arising from these elements are of particular interest because, unlike skeletal muscle which is associated with joints that limit degrees of freedom, caterpillar muscle is associated with a hydrostatic skeleton that affords nearly limitless degrees of freedom. Yet, the central nervous system of *Manduca* is a comparatively simple one, raising the question of whether some information processing is embedded in the passive properties of the muscle. This underscores the importance of a constitutive model describing these properties.

In this paper, we present experimental data of the ventral interior lateral (VIL) muscle of the *Manduca* in both the passive and the stimulated state. The muscle is subjected to periodic loading–unloading cycles to precondition the material for a reproducible stress–stretch response. During the first few cycles of repeated loading to the same displacement magnitude, stress softening occurs which is qualitatively similar to the Mullins effect in particle-reinforced natural rubber (Dorfmann & Ogden 2004).

The *Manduca* muscle is considered a nonlinear pseudo-elastic composite with an isotropic base material embedding a number of fibres. These introduce a preferred direction and the material is said to be transversely isotropic. During tetanic simulation, the fibres increase the cross-bridge formations between actin and myosin, which then induce an increase in the macroscopic material stiffness.

We start in §2 by showing similarities between the mechanical response of the *Manduca* muscle and carbon-black-reinforced natural rubber. It is shown that both the materials are capable of large nonlinear pseudo-elastic deformations and display stress softening during the first few cycles of periodic loading and unloading. In section 3, we summarize the basic equations of nonlinear elasticity of transversely isotropic materials, first for general deformations and then for the appropriate uniaxial specialization. An overview of the general theory of pseudo-elasticity, originally introduced by Ogden & Roxburgh (1999), is given next and adapted to capture uniaxial loading–unloading of transversely isotropic materials.

Section 4 contains a brief discussion on specimen preparation, measurement of the cross-sectional area and muscle stimulation. The experimental data for caterpillar muscle in the passive and the stimulated states demonstrate both the hysteretic response and stress softening. After four loading–unloading cycles, the stress–stretch response becomes stabilized. In section 5, we use the theory of §3 to develop a model for the *Manduca* muscle in the passive and the stimulated states. The reproducible stress–stretch response is used to determine material parameters and a good agreement with the presented data is shown.

2. SIMILARITIES BETWEEN SOFT BIOLOGICAL TISSUE AND RUBBER

The mathematical foundations first developed to characterize the highly nonlinear behaviour of unfilled and carbon-black-reinforced rubber have been successfully adapted to describe the mechanical response of biological tissue. The mechanical response of both the materials is qualitatively similar. Both are capable of large nonlinear pseudo-elastic deformations and display stress softening during the first few cycles of repeated loading to the same displacement magnitude. However, there is an important difference. Biological tissue is composed of an isotropic matrix embedding multiple oriented families of protein fibres. Therefore, the material response is best described as anisotropic. Rubber response, on the other hand, is generally isotropic.

Pseudo-elastic solids have been defined by Fung (1980) as materials with a hysteretic characteristic when subjected to cyclic loading and unloading, i.e. the loading–unloading responses do not coincide, even though the body returns to its original state. The material is considered an elastic material during loading and a different elastic material during unloading. The pseudo-elastic behaviour of a biological material and the response of a carbon-black-reinforced natural rubber compound during loading and unloading are shown in figure 1.

When an unfilled or carbon-black-reinforced rubber is subjected to cyclic loading with a fixed amplitude from its initial natural configuration, the stress required on reloading is less than that on the initial loading for elongations up to the maximum elongation achieved. The stress differences in successive loading cycles are largest during the first and second cycles and become negligible after *ca* 6–10 cycles, depending on the amount of filler and maximum extension. When this happens, the material loading–unloading response is said to have stabilized. Subsequent loading–unloading occurs along the stabilized path as long as the maximum deformation (alternatively called the level of preconditioning) is not exceeded. This phenomenon is known as the Mullins effect and described in detail by Dorfmann & Ogden (2004) and Horgan *et al.* (2004). Similarly, for biological materials, it is necessary to perform a number of loading–unloading cycles to precondition the material for a repeatable and predictable stress–strain response.

Figure 2 illustrates some of these similarities by comparing data from uniaxial tension tests of carbon-black-filled natural rubber and non-stimulated (passive) muscles harvested from the caterpillar *Manduca*. To monitor the progression of stress softening and to determine the ultimate stress–deformation response, periodic loading, unloading and reloading

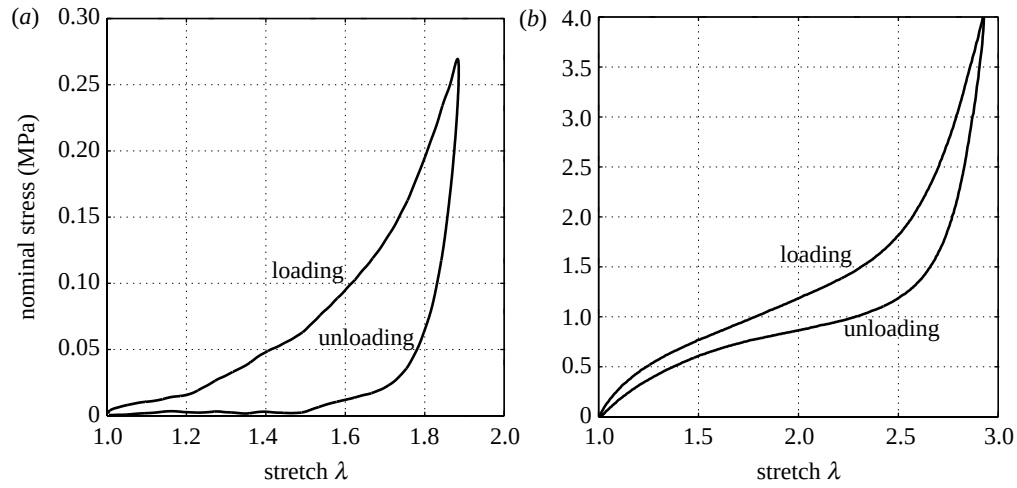

Figure 1. Pseudo-elastic response of a preconditioned *Manduca* muscle (*a*) and of a carbon-black-reinforced natural rubber specimen (*b*).

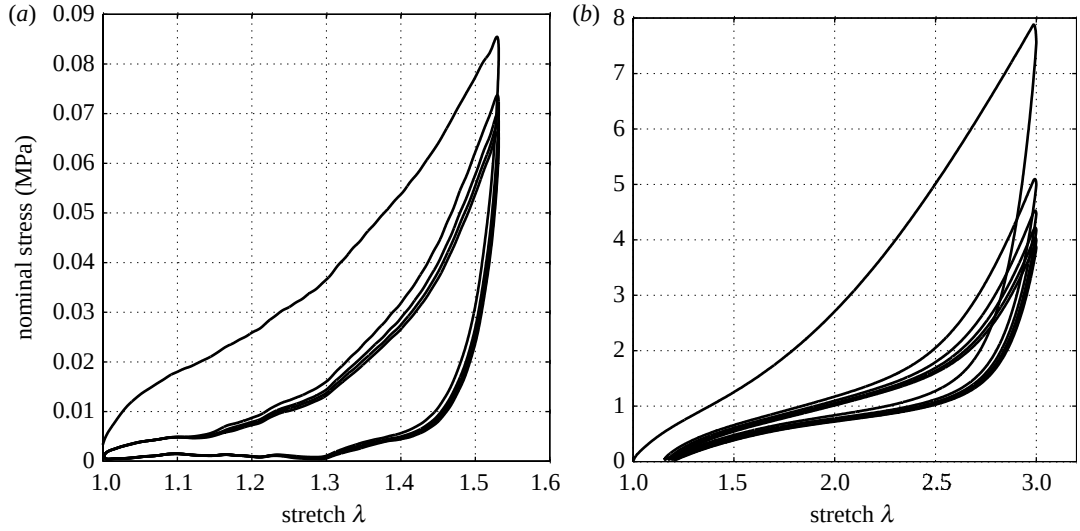

Figure 2. Preconditioning of a passive caterpillar muscle (*a*) and a carbon-black particle-reinforced rubber specimen (*b*) with maximum stretches $\lambda = 1.53$ and 3, respectively.

tests were performed at constant strain rate and at constant temperature of 25°C. During the first series of tests, a single muscle from the caterpillar was subjected to four cycles of preconditioning up to a pre-selected stretch $\lambda = 1.53$. The filled natural rubber specimen was subjected to six loading–unloading cycles up to a maximum stretch of $\lambda = 3$. The results, reported as nominal stress versus stretch λ in figure 2, show that the stress–stretch responses of the biological tissue and the natural rubber compound are qualitatively similar, even though they differ in strength and stiffness as expected. In the second series of experiments, an additional muscle from a caterpillar and an additional natural rubber specimen were each subjected to periodic loading up to two different, but fixed, stretches. The biological tissue was subjected to four loading–unloading cycles up to $\lambda = 1.2$ and the natural rubber specimen to six cycles up to $\lambda = 1.5$. After completion of the unloading cycles, each specimen was then loaded to a stretch of $\lambda = 1.4$ ($\lambda = 2$) and again subjected to four (six) cycles. A comparison of these results in figure 3 shows that the stress–stretch responses are again qualitatively similar. An apparent difference is the relative amount of energy dissipated during cyclic loading. For the present choices of test specimens, the difference between energy input during loading and energy returned during unloading is larger for the biological tissue.

The pioneering investigation by Wöhlisch (1926) first addressed similarities between natural rubber and biological tissues, even though he recognized the widely different chemical constitutions. In particular, Wöhlisch used the phenomenon of thermal agitation of long-chain molecules to explain the contraction of tendons and of stretched natural rubber specimens on heating. Wöhlisch used these important findings to replace the concept of rigid molecular structures with flexible long-chain molecules capable of internal vibrations and rotations owing to thermal fluctuations. Wöhlisch concluded that the elastic force in the material is owing to thermal motion of long, flexible and partially stretched chain molecules. The molecular explanation of the thermoelastic behaviour of rubber and biological tissue was also given by Meyer *et al.* (1932).

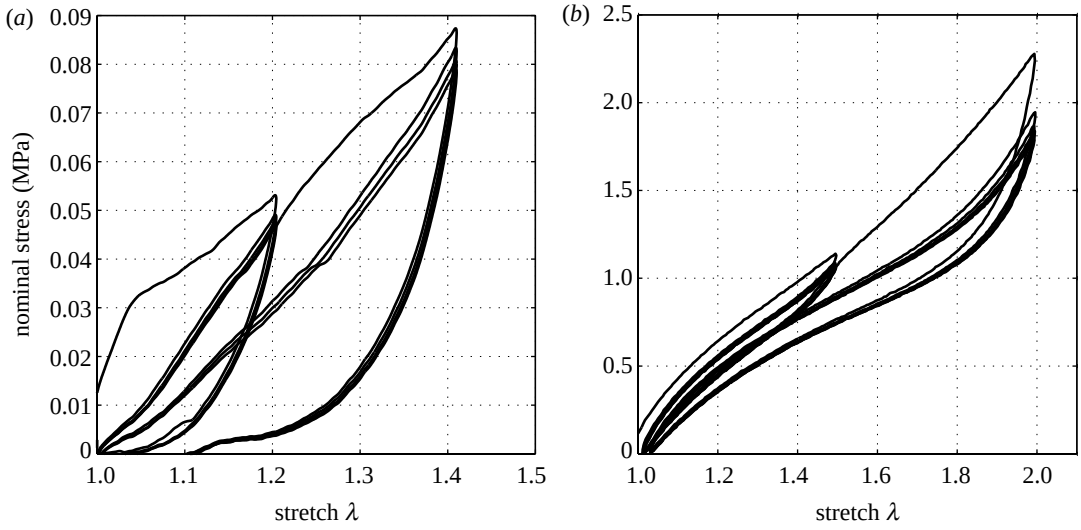

Figure 3. Periodic uniaxial extension tests of a passive caterpillar muscle (*a*) and a particle-reinforced rubber specimen (*b*) with two different but constant maximum elongations.

In particular, Meyer *et al.* (1932) pointed out that the motion of a molecular segment is influenced by the movement of neighbouring groups and independent of the movement of molecular segments further away. They also introduced the concept of statistically determined configurations of molecular chains and determined that the probability of assuming a folded or crumpled configuration is much higher than a straight form. In other words, there is only one straight but many twisted configurations that are possible (Meyer 1952). The possibility that a long-chain molecule assumes a statistically determined configuration and the exchange of energy with surrounding atoms are now fully accepted and are referred to as the kinetic theory of rubber elasticity.

The correspondence between rubber-like solids and muscles was first observed by Karrer (1933). Karrer regarded both materials as having a network of macromolecules bridged by permanent and/or temporary cross-links or junctions, entanglements and van der Waals forces. In a simplistic representation, the position and the number of these cross-links are not fixed, but are assumed to alter under loading, resulting in transient networks. As a consequence, the behaviour of such materials is different from, for example, metals where an ordered assembly of atoms is bonded by strong interatomic forces to form a relatively rigid structure. The concept of kinetic theory of rubber elasticity and the similarities of the pseudo-elastic behaviour of natural rubber and muscle fibres are also described in detail in the monograph by Treloar (2005). These similarities support the use of recent advances in theoretical and computational modelling of rubber-like solids to the field of biomechanics of soft tissue.

3. BASIC EQUATION

3.1. Kinematics

We consider the *Manduca* muscle as a pseudo-elastic body, which in its unstressed configuration is not stimulated and not subjected to any mechanical loads. Let the region in the three-dimensional Euclidean space occupied by the muscle in this configuration be denoted $\mathcal{B}_0$, i.e. the natural configuration of the muscle in the animal. For the passive as well as the stimulated muscle, we take the geometric configuration $\mathcal{B}_0$ to be the reference configuration from which to measure any subsequent deformation generated by the application of mechanical loads. The geometric configuration $\mathcal{B}_0$ for a change in stimulation can be maintained, if necessary, if appropriate mechanical loads are applied.

We denote by $\boldsymbol{X}$ the position vector of a material point within the body in the reference configuration $\mathcal{B}_0$ relative to an arbitrary chosen origin. Suppose the application of mechanical loads deform the body, so that the point $\boldsymbol{X}$ occupies the new position $\boldsymbol{x}=\boldsymbol{\chi}(\boldsymbol{X})$ in the time-independent deformed configuration, which we denote by $\mathcal{B}$. The vector field $\boldsymbol{\chi}$, which is a one-to-one, orientation-preserving mapping with suitable regularity properties, describes the deformation of the body.

The deformation gradient tensor F relative to $\mathcal{B}_0$, and its determinant, is

$$\mathsf{F} = \operatorname{Grad} \boldsymbol{\chi}, \qquad J = \det \mathsf{F} > 0, \tag{3.1}$$

where Grad denotes the gradient operator with respect to $\boldsymbol{X}$ and wherein the notation J is defined. Denote by $\mathrm{d}V$ and $\mathrm{d}v$ volume elements in $\mathcal{B}_0$ and $\mathcal{B}$, respectively, then we have the relation

$$\mathrm{d}v = J\,\mathrm{d}V, \tag{3.2}$$

and for a volume preserving (isochoric) deformation $J=\det \mathsf{F}=1$. The Cartesian components of F are given by $F_{ij}=\partial x_i/\partial X_j$, where X_i and x_i, $i=1, 2, 3$, are the Cartesian components of $\boldsymbol{X}$ and $\boldsymbol{x}$, respectively. For a detailed discussion on the kinematics of continua, we refer to, for example, Ogden (1997) and Holzapfel (2001).

The unique polar decompositions of the deformation gradient F are

$$\mathsf{F} = \mathsf{RU} = \mathsf{VR}, \tag{3.3}$$

where R is a proper orthogonal tensor; and U and V are positive definite and symmetric, respectively, the right and the left stretch tensors. These can be expressed in spectral form. For U, for example, we have the spectral decomposition

$$\mathsf{U} = \sum_{i=1}^{3} \lambda_i \boldsymbol{u}^{(i)} \otimes \boldsymbol{u}^{(i)}, \tag{3.4}$$

where the principal stretches $\lambda_i > 0$, $i \in \{1, 2, 3\}$, are the eigenvalues of U; $\boldsymbol{u}^{(i)}$ are the (unit) eigenvectors of U; and $\otimes$ denotes the tensor product. For incompressible materials,

$$J = \det \mathsf{F} = \lambda_1 \lambda_2 \lambda_3 \equiv 1. \tag{3.5}$$

Using the polar decomposition (3.3), we define

$$\mathsf{C} = \mathsf{F}^{\mathrm{T}}\mathsf{F} = \mathsf{U}^2, \qquad \mathsf{B} = \mathsf{F}\mathsf{F}^{\mathrm{T}} = \mathsf{V}^2, \tag{3.6}$$

which denote the right and the left Cauchy–Green deformation tensors, respectively. The three principal invariants of C, equivalently B, are defined by

$$\begin{aligned} I_1 &= \operatorname{tr} \mathsf{C}, \qquad I_2 = \frac{1}{2}[(\operatorname{tr} \mathsf{C})^2 - \operatorname{tr}(\mathsf{C}^2)], \\ I_3 &= \det \mathsf{C} = J^2, \end{aligned} \tag{3.7}$$

where tr is the trace of a second-order tensor.

Throughout the following work, we use the term 'fibre' in the mechanical sense. In muscles, this will include actin, myosin and other proteins arranged uniaxially. In a macroscopic sense, the *Manduca* muscle has therefore a single preferred direction and can be regarded as transversely isotropic. Let the directional reinforcement provided by the fibres be defined by the unit vector $\boldsymbol{A}$ in the undeformed configuration. Additional invariants, denoted I_4 and I_5, are associated with the fibre direction and are given by

$$I_4 = \boldsymbol{A} \cdot \mathsf{C}\boldsymbol{A} = \mathsf{F}\boldsymbol{A} \cdot \mathsf{F}\boldsymbol{A} = \boldsymbol{a} \cdot \boldsymbol{a}, \tag{3.8}$$

$$I_5 = \boldsymbol{A} \cdot \mathsf{C}^2 \boldsymbol{A} = \boldsymbol{a} \cdot \mathsf{B}\boldsymbol{a}, \tag{3.9}$$

where we introduced the notation $\boldsymbol{a} = \mathsf{F}\boldsymbol{A}$ to define the mapping of $\boldsymbol{A}$ under the deformation F.

There is a simple geometric interpretation of the invariant I_4. The square root of I_4 provides changes in the length of the fibre in the direction $\boldsymbol{A}$. Let, for example, the fibre in the undeformed configuration be directed along the unit vector $\boldsymbol{i}_1$, where $\boldsymbol{i}_1$, $\boldsymbol{i}_2$, $\boldsymbol{i}_3$ are the rectangular Cartesian basis vectors, then $I_4 = C_{11}$. If the fibre direction $\boldsymbol{A}$ is again taken in the $\boldsymbol{i}_1$ direction, then $I_5 = C_{11}^2 + C_{12}^2 + C_{13}^2$. The invariant I_5, by means of C_{11}, represents the changes in the length in the fibre direction and additionally, by means of C_{12} and C_{13}, shear deformation.

3.2. Constitutive equations

Let the unit vector $\boldsymbol{A}$ be a preferred direction in the reference configuration $\mathcal{B}_0$. The material response is indifferent to an arbitrary rotation about the direction $\boldsymbol{A}$. Also the material response is not altered by a change of direction from $\boldsymbol{A}$ to $-\boldsymbol{A}$. Following the analysis of such materials given in Spencer (1971) and Ogden (2001*a*), for example, we define a transversely isotropic material as one for which the strain energy, denoted W, is an isotropic function of the two tensors F and $\boldsymbol{A} \otimes \boldsymbol{A}$. The form of W is then reduced to dependence on the five independent invariants I_1, I_2, …, I_5 and we write

$$W = W(I_1, I_2, I_3, I_4, I_5). \tag{3.10}$$

Restricting attention to incompressible materials with $I_3 \equiv 1$, the strain energy is then a function of the remaining four invariants. The response of a constrained transversely isotropic material, with fibre direction corresponding to $\boldsymbol{A}$ in the reference configuration, is given by the nominal stress $\mathbf{S}$ and the Cauchy stress $\boldsymbol{\sigma}$. They are given, respectively, by

$$\mathbf{S} = \frac{\partial W}{\partial \mathsf{F}} - p\mathsf{F}^{-1}, \qquad \boldsymbol{\sigma} = \mathsf{F}\frac{\partial W}{\partial \mathsf{F}} - p\mathbf{I}, \tag{3.11}$$

where p is a Lagrange multiplier associated with the constraint (3.5). To write the explicit forms of $\mathbf{S}$ and $\boldsymbol{\sigma}$, we use the formulae

$$\frac{\partial I_1}{\partial \mathsf{F}} = 2\mathsf{F}^{\mathrm{T}}, \qquad \frac{\partial I_2}{\partial \mathsf{F}} = 2(I_1 \mathsf{F}^{\mathrm{T}} - \mathsf{F}^{\mathrm{T}}\mathsf{F}\mathsf{F}^{\mathrm{T}}), \tag{3.12}$$

$$\frac{\partial I_4}{\partial \mathsf{F}} = 2\boldsymbol{A} \otimes \mathsf{F}\boldsymbol{A}, \qquad \frac{\partial I_5}{\partial \mathsf{F}} = 2(\boldsymbol{A} \otimes \mathsf{F}\mathsf{C}\boldsymbol{A} + \mathsf{C}\boldsymbol{A} \otimes \mathsf{F}\boldsymbol{A}). \tag{3.13}$$

A direct calculation then leads to

$$\begin{aligned} \mathbf{S} = {} & 2(W_1 + I_1 W_2)\mathsf{F}^{\mathrm{T}} - 2W_2 \mathsf{C}\mathsf{F}^{\mathrm{T}} + 2W_4 \boldsymbol{A} \otimes \mathsf{F}\boldsymbol{A} \\ & + 2W_5(\boldsymbol{A} \otimes \mathsf{F}\mathsf{C}\boldsymbol{A} + \mathsf{C}\boldsymbol{A} \otimes \mathsf{F}\boldsymbol{A}) - p\mathsf{F}^{-1}, \end{aligned} \tag{3.14}$$

$$\begin{aligned} \boldsymbol{\sigma} = {} & 2(W_1 + I_1 W_2)\mathsf{B} - 2W_2 \mathsf{B}^2 + 2W_4 \boldsymbol{a} \otimes \boldsymbol{a} \\ & + 2W_5(\boldsymbol{a} \otimes \mathsf{B}\boldsymbol{a} + \mathsf{B}\boldsymbol{a} \otimes \boldsymbol{a}) - p\mathbf{I}. \end{aligned} \tag{3.15}$$

When the dependence on I_4 and I_5 in equations (3.14) and (3.15) is omitted, the associated expressions for an isotropic material are obtained.

For fibre-reinforced materials, it is common to write the strain-energy function as the sum of two terms, one associated with the isotropic properties of the base matrix and the second to introduce transverse isotropy in the mechanical response. We therefore consider a strain-energy function given by

$$W = W_{\mathrm{iso}}(I_1, I_2) + W_{\mathrm{fib}}(I_4, I_5), \tag{3.16}$$

where the term W_{iso} represents the isotropic matrix material and W_{fib} accounts for the directional reinforcement, the latter also known as the reinforcing model (Qiu & Pence 1997; Merodio & Ogden 2003). We consider, following Qiu & Pence (1997) and Merodio & Ogden (2005), an incompressible neo-Hookean material augmented with a reinforcing model that depends only on I_4 and has the form

$$W = \frac{1}{2}\mu[(I_1 - 3) + \mu_{\mathrm{e}}(I_4 - 1)^2]. \tag{3.17}$$

The shear modulus of the base material is denoted by μ and the strength of the reinforcement in the fibre direction is given by μ_{e}. For the strain-energy function (3.17), both the strain energy and the stress vanish in the undeformed configuration.

The experimental data in §4 show that the muscle of *Manduca* is subjected to uniaxial loading–unloading in the fibre direction. Therefore, we are interested in the

response of an incompressible transversely isotropic material under simple deformations in the fibre direction.

3.2.1. Uniaxial loading in the fibre direction. In the simple tension (or compression) specialization, we take the principal stretches $\lambda_2=\lambda_3$ and use the notation

$$\lambda_1 = \lambda, \qquad \lambda_2 = \lambda^{-1/2}, \tag{3.18}$$

satisfying the incompressibility condition (3.5). From equations (3.7) and (3.8), we have

$$I_1 = \lambda^2 + 2\lambda^{-1}, \qquad I_4 = \lambda^2, \tag{3.19}$$

and the strain energy then depends on the one remaining independent stretch, which we denote by $\hat{W}(\lambda)$ and write

$$\hat{W}(\lambda) = W(I_1, I_4). \tag{3.20}$$

Writing the strain energy (3.17) as a function of λ, we obtain

$$\hat{W}(\lambda) = \frac{1}{2}\mu[(\lambda^2 + 2\lambda^{-1} - 3) + \mu_e(\lambda^2 - 1)^2]. \tag{3.21}$$

In this case, the only non-zero stress component is in the fibre direction and $\sigma_2=\sigma_3=0$. The Cauchy stress associated with λ is

$$\sigma = \sigma_1 = \lambda\frac{\mathrm{d}\hat{W}(\lambda)}{\mathrm{d}\lambda} = \mu(\lambda^2 - \lambda^{-1}) + 2\mu\mu_e(I_4 - 1)I_4. \tag{3.22}$$

3.3. Pseudo-elasticity

The theory of pseudo-elasticity, originally developed by Ogden & Roxburgh (1999) to account for the Mullins effect in carbon-black-reinforced elastomers, modifies the elastic strain-energy function $W(\mathsf{F})$ by incorporating an additional variable η. Thus, we write

$$W = W(\mathsf{F}, \eta). \tag{3.23}$$

The inclusion of η provides a means of changing the form of the energy function during the deformation process and hence changing the character of the stress–stretch response. In general, the response of the material is then no longer elastic and $W(\mathsf{F},\eta)$ is referred to as a *pseudo-energy* function. In this section, we provide an overview of the main ingredients of the general theory of pseudo-elasticity. Appropriate specifications are made in §5.

The variable η may be inactive or active; activating η introduces a change in the material properties. A change from inactive to active may be induced, for example, when unloading is initiated.

If the variable η is inactive, we set it to the constant value unity and write

$$W_0(\mathsf{F}) = W(\mathsf{F}, 1), \tag{3.24}$$

for the resulting strain-energy function. In equation (3.24) and in what follows, the zero subscript is associated with the situation in which η is inactive. For an incompressible material, the nominal stress associated with inactive η, denoted $\mathbf{S}_0$, is given by

$$\mathbf{S}_0 = \frac{\partial W_0}{\partial \mathsf{F}}(\mathsf{F}) - p_0\mathsf{F}^{-1}, \qquad \det\mathsf{F} = 1. \tag{3.25}$$

If η is active, we take it to depend on the deformation F. The nominal stress is then given by

$$\mathbf{S} = \frac{\partial W}{\partial \mathsf{F}}(\mathsf{F}, \eta) + \frac{\partial W}{\partial \eta}(\mathsf{F}, \eta)\frac{\partial \eta}{\partial \mathsf{F}}(\mathsf{F}) - p\mathsf{F}^{-1}, \tag{3.26}$$

$$\det\mathsf{F} = 1.$$

Following Ogden & Roxburgh (1999), we take η to be given implicitly by the constraint

$$\frac{\partial W}{\partial \eta}(\mathsf{F}, \eta) = 0, \tag{3.27}$$

which uniquely defines η in terms of F. We may write the solution to equation (3.27) formally as

$$\eta = \eta_e(\mathsf{F}). \tag{3.28}$$

Then, the expression of the nominal stress (3.26) simplifies and is given by

$$\mathbf{S} = \frac{\partial W}{\partial \mathsf{F}}(\mathsf{F}, \eta) - p\mathsf{F}^{-1}, \qquad \det\mathsf{F} = 1, \tag{3.29}$$

whether or not η is active, where, when η is active, the right-hand side is evaluated for η given by equation (3.28). It is convenient to introduce the notation w for the resulting (unique) strain-energy function. Thus,

$$w(\mathsf{F}) \equiv W(\mathsf{F}, \eta_e(\mathsf{F})), \tag{3.30}$$

and the nominal and Cauchy stress tensors for incompressible materials are given by the standard relations

$$\mathbf{S} = \frac{\partial w}{\partial \mathsf{F}}(\mathsf{F}) - p\mathsf{F}^{-1}, \qquad \boldsymbol{\sigma} = \mathsf{F}\frac{\partial w}{\partial \mathsf{F}}(\mathsf{F}) - p\mathbf{I}. \tag{3.31}$$

Thus far, we have not specified the form of the dependence of W on η, or, more particularly, the form of the function $\eta_e(\mathsf{F})$ in equation (3.28).

3.3.1. Uniaxial loading–unloading in the fibre direction. When specialized to transversely isotropic materials subject to uniaxial loading–unloading in the fibre direction, we take $\sigma_2=\sigma_3=0$ and write $\sigma_1=\sigma$. Similar to §3.2.1, we denote $\lambda_1=\lambda$, the principal stretch in the fibre direction and $\lambda_2=\lambda_3=\lambda^{-1/2}$.

The modified energy in equation (3.20) becomes

$$\hat{W}(\lambda, \eta) = W(I_1, I_4, \eta), \tag{3.32}$$

and for inactive η from equation (3.24), we have the expression

$$\hat{W}_0(\lambda) = \hat{W}(\lambda, 1). \tag{3.33}$$

The associated Cauchy stress for inactive η is given by

$$\sigma_0 = \lambda\frac{\mathrm{d}\hat{W}_0}{\mathrm{d}\lambda}(\lambda), \tag{3.34}$$

and for active η, it has the form

$$\sigma = \lambda\frac{\partial \hat{W}}{\partial \lambda}(\lambda, \eta). \tag{3.35}$$

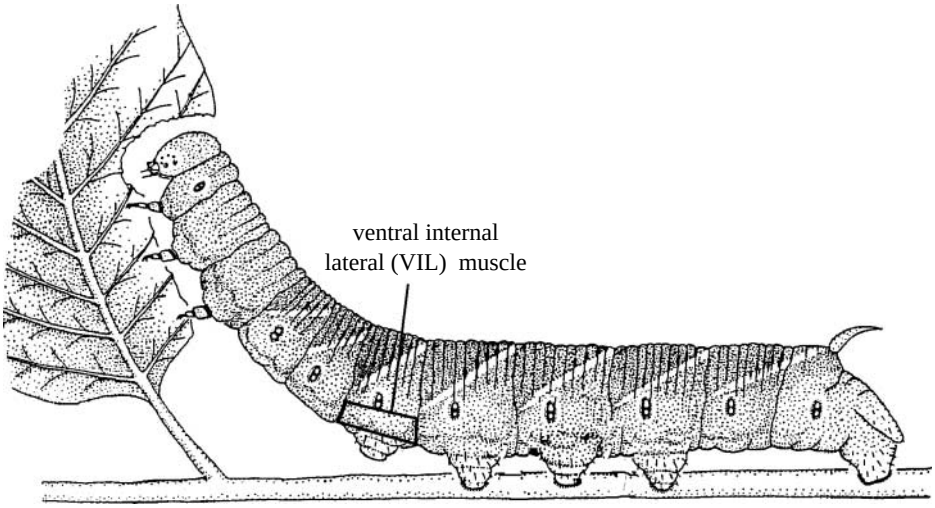

Figure 4. A fifth instar *Manduca sexta* caterpillar illustrating the position of the ventral internal lateral muscle in the third abdominal body segment.

Equation (3.27) is modified and we obtain

$$\frac{\partial \hat{W}}{\partial \eta}(\lambda, \eta) = 0, \tag{3.36}$$

which can be solved explicitly for η. This relation, using the notation from equation (3.28), has the form

$$\eta = \eta_{\mathrm{e}}(\lambda). \tag{3.37}$$

Following equation (3.30), we obtain the energy function for active η. Using the notation $\hat{w}(\lambda)$, we have

$$\hat{w}(\lambda) = \hat{W}(\lambda, \eta_{\mathrm{e}}(\lambda)), \tag{3.38}$$

and the Cauchy stress in the loading direction for inactive and active η is given by

$$\sigma = \lambda \frac{\mathrm{d}\hat{w}}{\mathrm{d}\lambda}(\lambda). \tag{3.39}$$

The theory of pseudo-elasticity outlined earlier and described in more detail by Ogden & Roxburgh (1999) and Ogden (2001*b*) is a very general framework and allows considerable flexibility in the choice of specific models.

4. EXPERIMENTAL RESULTS

Since *Manduca* lacks a stiff skeleton, its muscles are attached directly to infoldings of the body wall (apodemes). The muscles are organized in repeated segments along the body length and in several overlapping layers. As with all striated muscles, their activity is controlled by depolarization-initiated release of transmitters from motor nerve terminals. The amount, and time course, of transmitter release is a function of the pattern and frequency of action potentials in the motor neuron. Trains of action potentials (tetany) stimulate muscles to develop force, or to shorten, by cycling cross-bridge formation between actin and myosin myofilaments (Huxley 2000*a*). During each step of a crawl in *Manduca*, the VIL in each body segment is activated by a brief burst (less than 1 s) of action potentials with a mean frequency of *ca* 20 Hz. During other movements, the muscle can be activated by bursts of action potentials at 30–40 Hz for several seconds. In this paper, we will model the muscle both in its unstimulated (passive) state and during a sustained tetanic stimulation.

4.1. Muscle preparation

To assess preconditioning, pseudo-elasticity and stiffening owing to stimulation, a series of periodic uniaxial extension tests were carried out on VIL of the third abdominal segment of larval *Manduca*.

Following the method described by Bell & Joachim (1976), larvae were raised on an artificial diet at 26°C under long-day conditions (17 h light/7 h dark). Animals on the second day of the fifth instar were used for testing using the following procedure:

(i) Preliminary dissections were made to map the location of the attachment points of the muscle, VIL, in the third abdominal segment to exterior markers (figure 4).
(ii) Animals were anaesthetized by chilling on ice, and the length of VIL was measured using the markers determined in step (i). A full-length dorsal incision was made and the gut, head and posterior half of the terminal segment removed.
(iii) The cuticle, intact muscles and nerves were exposed in physiological saline, with the interior of the cuticle facing upward. During dissection, the saline was perfused with air approximately every 5 min.
(iv) VIL was dissected out leaving a small portion of attached cuticle at both ends.
(v) The two motor neurons innervating VIL, project through the dorsal nerve (Levine & Truman 1985). Therefore, the dorsal nerve and its segmental ganglion were kept intact, all other nerves were severed. The muscle was stimulated by applying bursts of supramaximal voltage pulses to the dorsal nerve using a suction electrode.
(vi) Experiments were completed within 2 h of the time of initial incision.

4.2. Measurement of cross-sectional area

Microscopic analyses of VIL revealed a total of 14 individual 4–5 mm long fibres. The direct measurement of the cross-sectional area of the muscle is either invasive or at least risks injury to the individual fibres. Therefore, we determined the undeformed cross-sectional area of the muscles using a relationship derived from invasive measurements of separate muscle preparations.

Since individual fibres are difficult to distinguish clearly in intact muscles, we removed fibres from resting-length single-muscle preparations until the remaining fibres could be clearly imaged from overhead. Since the fibres are not circular but rather elliptical in cross-section, an overhead image provides only the major axis dimension. We therefore imaged the cut ends of stained fibres teased into a vertical position. The dimensions were calculated in NIH ImageJ software using 169 µm diameter polymer beads for calibration (Duke Scientific Corp., Palo Alto, CA, USA) included in the images as a reference. The ratio of major to minor axis lengths was used to calculate cross-sectional area of fibres from overhead image dimensions. Mean cross-sectional area was multiplied by the number of fibres. The resulting value was used to calculate cross-sectional area of muscles used in strain cycling measurements from their resting length with the assumption that muscle proportions increased or decreased isometrically.

4.3. Muscle stimulation

During tetanic stimulation, VIL develops force comparatively slowly, reaching peak force up to several seconds after initiation of stimulus (figure 5). There is a considerable variation between preparations, with peak force rise time ranging from 1 to 6 s. Once reaching a peak value, force under sustained stimulation declines, again with much variation in time course between muscle preparations. Generally, preparations that develop force more slowly also sustained force more uniformly throughout the final 8 s of a 10 s tetanus. Initiating strain cycling 2 s after initiating stimulus allowed even more slowly contracting preparations to reach more than 90% of peak force before strain cycling began.

4.4. Strain cycling and force measurement

Muscles were pinned by the attached cuticle at each end in a horizontal bath of saline. One end was pinned to the edge of an elastomer platform in the bath, while the other was secured by a hook to an Aurora 300B-LR lever-arm ergometer (Aurora Scientific, Inc., Aurora, Ontario). The shaft of the hook and the movement of the lever arm were horizontal, and the hook was attached to the lever arm by a small tunnel of epoxy that allowed free movement of the hook only in the horizontal plane.

Bath temperature was maintained at 25°C by a thermostatically controlled Peltier device built into the stage supporting the bath. Saline was continuously exchanged and kept aerated.

Lever arm motion was controlled and force recorded by DMC software (Aurora Scientific, Inc.) via a National Instruments NiDaq 6024E interface. Lever arm position was updated at 1800 Hz and force and position were recorded at 2000 Hz. Data were filtered and exported in DMA software (Aurora Scientific, Inc.).

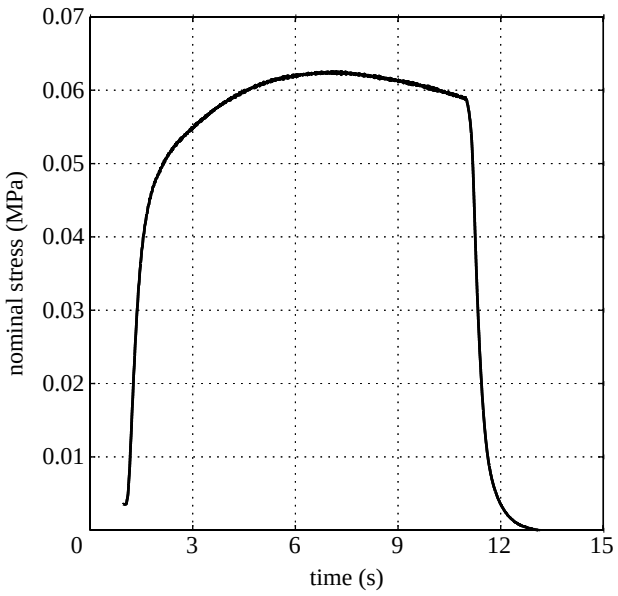

Figure 5. Time course of force developed by VIL *in vitro* held at the length measured in the resting animal and given a 10 s electrical stimulus via the muscle's motor neuron. In this preparation, from which the data in figure 6 were obtained, the stimulated muscle sustained greater than 90% of peak force for the final 8 s of the stimulus train, reaching a peak force 5.9 s after initiation of stimulus.

For measurements of VIL under tetanic stimulus, a suction electrode was applied to the dorsal nerve. Since peak force response time for VIL was 1.5–6 s, a supramaximal stimulus (40 volt, 40 Hz) was initiated 2 s before strain cycling began and sustained throughout strain cycling. The biological data shown here is a representative example of five tested specimens.

4.5. Experimental data

The contractile properties of striated muscles are similar across species. In general, muscle force is proportional to its cross-sectional area and speed is proportional to its length. Muscles also develop their greatest power at approximately one-third the maximum unloaded speed (Huxley 2000*b*). Force generation in most striated muscles is limited to a narrow range of movements (with strains of 10–20% being typical). This arises because overlap of thick and thin myofilaments decreases as the fibres stretch, while the Z-disc prevents actin and myosin from penetrating into adjacent sarcomeres during contraction (e.g. Holmes & Geeves 2000). This non-continuous nature of the axial fibres results in a narrow peak of maximum force development centred on the resting length of the muscle; on each side of this peak, the maximum stimulated isometric force is significantly less. It is likely that the gradual decrease in stiffness, seen during loading of stimulated VIL and shown in figure 6*b*, represents a progressive decrease in available overlap for cross-link formation. This interpretation is supported by the relatively linear loading stiffness of a passive muscle

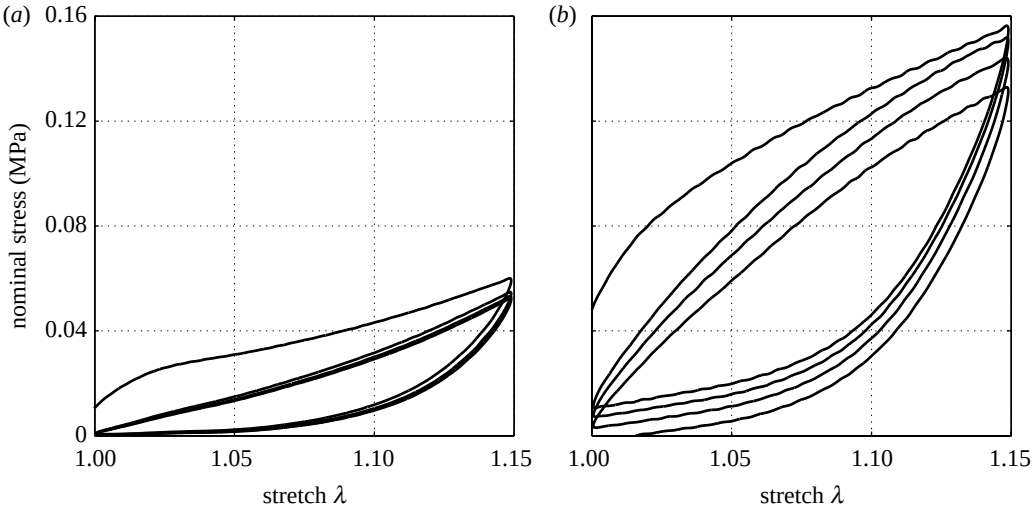

Figure 6. Preconditioning of a caterpillar muscle with maximum stretch of $\lambda=1.15$. (*a*) Results of a muscle in the passive state, while (*b*) for stimulated condition. Data for the stimulated condition were obtained during the final 8 s of a 10 s stimulus, corresponding to the period during which the same muscle preparation sustained force within 90% of peak values under tetanic isometric stimulation.

shown in figure 6*a*. In a passive muscle, bridge formation between actin and myosin would be expected to be minimal.

Interestingly, the loading hysteresis for VIL is not particularly large despite the application of a 15% strain. At least part of the explanation may lie in the extended range over which *Manduca* larval muscles can develop force. This ability is presumably an adaptation for long movements without the advantage of a rigid lever system. Larval muscles of holometabolous insects, such as *Manduca*, have several structural features which suggest that they are supercontracting (Goldstein & Burdette 1971; Hardie 1976; Rheuben & Kammer 1980; Duch *et al.* 2000; Royuela *et al.* 2000; Schwartz & Ruff 2002). For example, muscles in *Manduca* caterpillars are striated but have long sarcomeres, very high tetanus-to-twitch for ratios and much slower force development (Rheuben & Kammer 1980). They also develop force at lengths from 0.5 to 1.5 times resting length (Garmirian & Trimmer, unpublished work), a range associated with supercontracting muscles in tsetse flies, which have both supercontracting and non-supercontracting visceral muscles (Rice 1970). Although it is not known whether *Manduca* larval muscles have the perforated or incomplete Z-discs that characterize supercontracting muscle (Herrel *et al.* 2002), the Z-discs are at least described as 'poorly defined and irregularly arranged' (Rheuben & Kammer 1980). Supercontracting muscles are found in both vertebrates and invertebrates and are often associated with hydrostatic movements (Osborne 1967; Rice 1970; Candia Carnevali 2005).

One prediction of this interpretation of the deformation-dependent loading stiffness is that conventional striated (non-supercontracting) muscle will exhibit a more marked loading hysteresis when subjected to such large strain. This is because in striated muscle, the sarcomeres are aligned and the degree of actin and myosin overlap throughout the muscle will be determined directly by the degree of stretch. In contrast, in *Manduca* muscles, the sarcomeres are less distinct which could lead to a greater heterogeneity in fibre overlap.

5. NUMERICAL RESULTS

5.1. *A model for the* Manduca *muscle*

In this section, we modify the pseudo-elastic model that was used previously by Dorfmann & Ogden (2003) to describe loading, partial unloading and reloading of particle-reinforced rubber. The *Manduca* muscle is taken to be incompressible and transversely isotropic and we use a pseudo-energy function for simple tension in the form

$$\hat{W}(\lambda,\eta) = \eta\,\hat{W}_0(\lambda) + \phi(\eta), \tag{5.1}$$

where the function ϕ accounts for the energy dissipated during a loading–unloading cycle. For consistency with equation (3.33), the function ϕ, for inactive η, must satisfy the condition $\phi(1)=0$. Using the expression of the reinforcing model for uniaxial loading in the fibre direction (3.21), equation (5.1) with $\eta\equiv 1$ has the form

$$\hat{W}_0(\lambda) = \hat{W}(\lambda,1) = \frac{1}{2}\mu[(\lambda^2+2\lambda^{-1}-3) + \mu_{\mathrm{e}}(\lambda^2-1)^2], \tag{5.2}$$

where μ_{e} describes the increase in strength of the fibres owing to tetanic stimulation, which also depends on the amount of extension λ, i.e. $\mu_{\mathrm{e}}=\mu_{\mathrm{e}}(\lambda)$. The associated Cauchy stress is then given by

$$\sigma_0 = \lambda\frac{\mathrm{d}\,\hat{W}_0(\lambda)}{\mathrm{d}\lambda} = \mu(\lambda^2-\lambda^{-1}) + \mu\lambda^2(\lambda^2-1) \times\left(2\mu_{\mathrm{e}} + \frac{\lambda^2-1}{2\lambda}\frac{\mathrm{d}\mu_{\mathrm{e}}}{\mathrm{d}\lambda}\right), \tag{5.3}$$

where the subscript '0' has been attached to $\hat{W}$ and σ to indicate that these expressions are used to describe the loading path.

Unloading may take place from any point on the loading path. The start of unloading is taken as

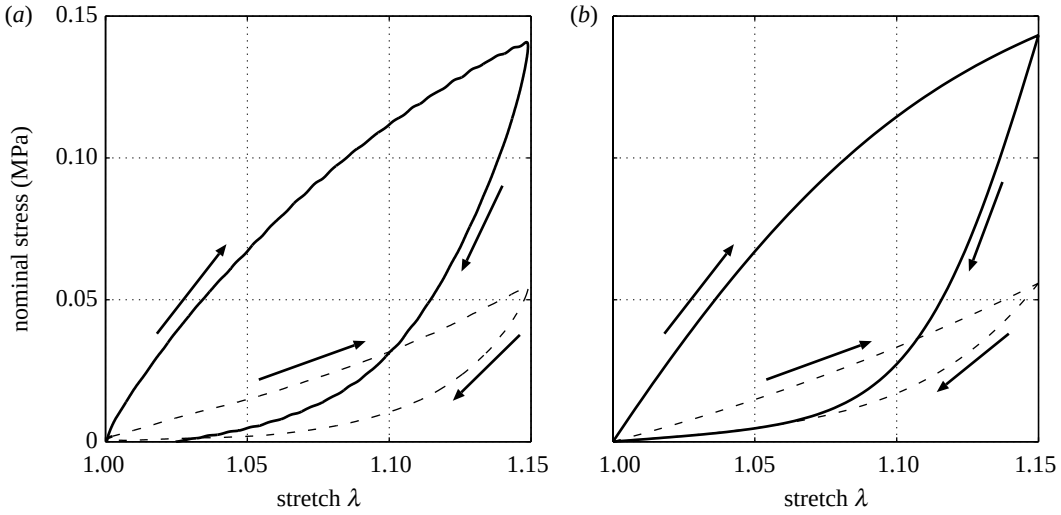

Figure 7. Experimental data (*a*) and numerical data (*b*) for preconditioned loading–unloading response of *Manduca* muscle in passive (dashed line) and stimulated (solid line) conditions.

the signal for η to be active and to change the form of the energy function. The Cauchy stress during unloading is then given by

$$\sigma = \eta\lambda\frac{\mathrm{d}\hat{W}_0}{\mathrm{d}\lambda}(\lambda) = \eta\sigma_0, \tag{5.4}$$

which shows that stress softening during unloading requires that $\eta \leq 1$, with equality only at the point where unloading is initiated. The dependence of $\hat{W}$ on η is given by equation (3.36) and has the form

$$\phi'(\eta) = -\hat{W}_0(\lambda). \tag{5.5}$$

It is important to point out that the value of η derived from equation (5.5) depends on the value of the principal stretch λ_m attained on the loading path, as well as on the specific forms of $\hat{W}_0(\lambda)$ and $\phi(\eta)$ employed. Since $\eta = 1$ at any point on the loading path from which unloading is initiated, it follows from equations (5.1) and (5.5) that

$$\phi'(1) = -\hat{W}_0(\lambda_\mathrm{m}) \equiv -\hat{W}_\mathrm{m}, \tag{5.6}$$

wherein the notation $\hat{W}_\mathrm{m}$ is defined. This is the current maximum value of the energy achieved on the loading path. In accordance with the properties of $\hat{W}_0$, $\hat{W}_\mathrm{m}$ increases along a loading path. In view of equation (5.6), the function ϕ depends on the point from which unloading begins through the energy expended on the loading path up to that point.

When the material is fully unloaded, with $\lambda = 1$, η attains its minimum value η_min. This is determined by inserting these values into equation (5.5) to give

$$\phi'(\eta_\mathrm{min}) = -\hat{W}_0(1) = 0, \tag{5.7}$$

where we assumed that no elastic energy is stored in the reference configuration corresponding to $\lambda = 1$. The residual (non-recoverable) energy $\phi(\eta_\mathrm{min})$ is given by equation (5.1) and has the value

$$\hat{W}(1, \eta_\mathrm{min}) = \phi(\eta_\mathrm{min}). \tag{5.8}$$

This may be interpreted as a measure of the energy dissipated in the muscle during the loading–unloading cycle. In simple tension, $\phi(\eta_\mathrm{min})$ is the area between the loading and the unloading curves. It is therefore appropriate to refer to ϕ as a *dissipation function*. Following Dorfmann & Ogden (2003), we select the function ϕ to have the form

$$-\phi'(\eta) = m\tanh^{-1}[r(\eta - 1)] + \hat{W}_\mathrm{m}, \tag{5.9}$$

where r and m/μ are dimensionless positive material parameters, μ being the shear modulus of the matrix material. The explicit form of η is obtained from equations (5.9) and (5.5) and has the form

$$\eta = 1 - \frac{1}{r}\tanh\left[\frac{\hat{W}_\mathrm{m} - \hat{W}_0(\lambda)}{m}\right]. \tag{5.10}$$

The variable η assumes the minimum value η_min when $\lambda = 1$, which corresponds to the natural configuration of the muscle in the animal. It is given by

$$\eta_\mathrm{min} = 1 - \frac{1}{r}\tanh\left[\frac{\hat{W}_\mathrm{m}}{m}\right]. \tag{5.11}$$

Finally, integration of equation (5.9) gives the dissipation explicitly in terms of the variable η in the form

$$\phi(\eta) = -m(\eta - 1)\tanh^{-1}[r(\eta - 1)] - \hat{W}_\mathrm{m}(\eta - 1) - \frac{m}{2r}\log[1 - r^2(\eta - 1)^2]. \tag{5.12}$$

5.2. A specific material model

We now apply the pseudo-elastic reinforcing model to simulate the passive as well as the stimulated loading–unloading response of the *Manduca* muscle shown in figure 6. Here, we assume that the material is preconditioned and the muscle characterized by the repeatable stress–stretch response. A detailed development, including experimental data, on preconditioning and recovery of the *Manduca* muscle will be given elsewhere.

The reproducible loading–unloading response of the muscle in the passive as well as the stimulated state is

Table 1. Summary of model parameters for loading and unloading of *Manduca* muscle in passive and active conditions.

material model parameters						
	μ (Pa)	c_1	c_2	c_3	r	m (Pa)
passive	755.5	86.13	0.0	0.53	1.05	0.0038
active	755.5	86.13	470.0	0.53	1.05	0.0038

shown in figure 7*a*. The maximum extension achieved is $\lambda = 1.15$ and the axial nominal stress is the applied load per unit undeformed cross-sectional area (equation (3.11)). Therefore, we are modelling the hysteresis associated with loading–unloading cycles and more particularly the effect of muscle stimulation on the macroscopic stiffness. The material is again taken to be incompressible and transversely isotropic.

The loading of the muscle in passive and stimulated conditions, shown in figure 7, is fully determined by the energy function (5.2). The value of the stiffness of the matrix material, denoted μ, is selected so that the numerical simulation was an appropriate match to the biological data and is given in table 1.

In equation (5.2), the variable μ_e is used to describe the change in strength of the actin and the myosin myofilaments owing to tetanic stimulation. For the test data shown in figure 7, we find that the increase in strength with increasing stimulation and the decrease with increasing λ may be given by

$$\mu_e = c_1 + c_2 e^{(1-\lambda^2)/c_3}, \tag{5.13}$$

where c_1, c_2 and c_3 are three dimensionless material constants. The constant c_1 with $c_2 = 0$ gives the stiffness of the muscle fibres in the passive state. The value of the constant c_2, which depends on the magnitude of stimulus, describes the increase in strength in the reference configuration. Finally, the constant c_3 describes the change in stimulus with deformation. We here omit the experimental evidence showing the reduction of the stimulus with deformation, since a separate development is in progress. The associated values are listed in table 1.

The unloading response of the muscle in the passive and the simulated state is given by equation (5.4) with η given by equation (5.10). The value of the constants r and m describing the hysteretic response are listed in table 1 and the associated numerical results shown in figure 7*b*. The fit of the model to the experimental data of the *Manduca* muscle in the passive and the stimulated state is good.

Figure 8 shows the pseudo-energy given by equation (5.1) and the amount of energy dissipated during cyclic loading of a *Manduca* muscle in passive and the stimulated conditions. On completion of the loading–unloading cycle, energy is dissipated and the energy returned upon complete unloading is less than the energy expended during loading. The amount of dissipated energy is the smallest for the passive muscle and increases with the amount of electric stimulus.

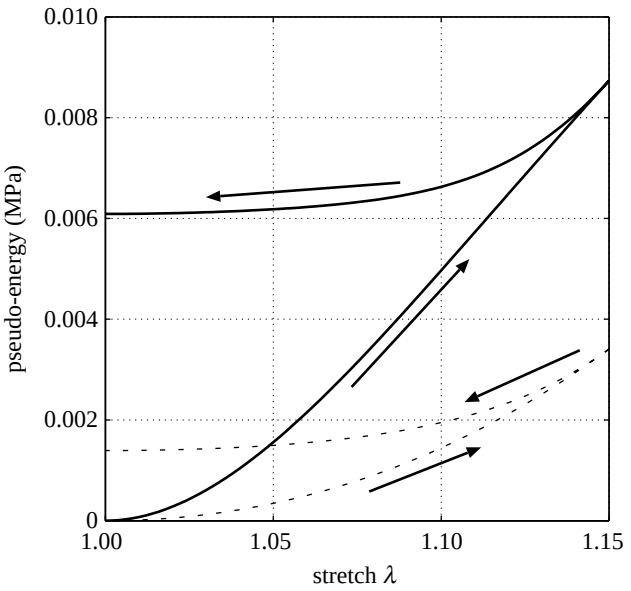

Figure 8. Plot of the pseudo-energy against the stretch during loading and unloading of passive (dashed line) and stimulated (solid line) *Manduca* muscle. The intercept of the unloading curves with the vertical axis quantifies the energy dissipated during one complete loading–unloading cycle.

6. CONCLUDING REMARKS

In this paper, we have presented new experimental data on the passive and stimulated response of the *Manduca* muscle. We have shown that the response is qualitatively similar to the loading–unloading behaviour of particle-reinforced rubber; both are capable of large nonlinear elastic deformations and stress softening during the first few cycles of periodic loading–unloading. Particle-reinforced rubber is, in general, an isotropic material; biological tissues, on the other hand, are composed of an isotropic base material reinforced with multiple families of protein fibres. The *Manduca* muscle is shown to have an isotropic base material reinforced with fibres that generates a transversely isotropic response with preferred direction along the loading direction.

The constitutive relation presented here and used to describe the response of the *Manduca* muscle in passive and stimulated conditions is based on an incompressible neo-Hookean material augmented with a reinforcing model, the latter being a function of the invariant I_4 (Qiu & Pence 1997; Merodio & Ogden 2005). A good agreement is obtained with the experimental data for both the passive and the stimulated conditions.

It has also been shown that the strength in the fibre direction, denoted by μ_e, depends on the amount of tetanic stimulation and deformation. Increasing stimulus provides for a greater strength in the actin and the myosin myofilaments. The strength parameter μ_e also accounts for the interaction between deformation and stimulus and it is shown that the effect of the stimulation reduces with increasing deformation. Experimental data in support of this important observation will be given elsewhere.

The interaction of the electrical stimulus and deformation in the *Manduca* muscle is similar to the behaviour of electro-sensitive materials (Dorfmann & Ogden 2005). Both are capable of increasing stiffness

during stimulation and the effect of the stimulus depends on the amount of deformation. A detailed study on this coupled phenomenon in the *Manduca* muscle is currently being performed and will be given elsewhere.

From a biological perspective, *Manduca* muscles have to serve many functions without the advantage of stiff levers and joints. The nonlinear mechanical properties described here for *Manduca* muscle are likely to have a profound effect on the way the nervous system controls movements. One possibility is that by 'exploiting' these complex muscle mechanics, the nervous system can reduce its computational load and thereby cope with the high-dimensional workspace, with many degrees of freedom, inherent in flexible structures. Such mechanical properties contribute to the functionality of locomotory muscle and associated tissue of more widely researched animals with hard skeletons and fewer degrees of freedom ranging from hexapods (Jindrich & Full 2002; Seipel *et al.* 2004; Dudek & Full 2006) to humans (Hof 2003). It is therefore important to include the pseudo-elastic characteristics of tissues when modelling the control of locomotory muscle, especially with soft-bodied animals.

REFERENCES

Bell, R. A. & Joachim, F. G. 1976 Techniques for rearing laboratory colonies of tobacco hornworms and pink bollworms Lepidoptera–Sphingidae–Gelechiidae. *Ann. Entomol. Soc. Am.* **69**, 365–373.

Biewener, A. A. 2003 *Animal locomotion*. New York, NY: Oxford University Press.

Biewener, A. A. & Roberts, T. J. 2000 Muscle and tendon contributions to force, work, and elastic energy savings: a comparative perspective. *Exerc. Sport Sci. Rev.* **28**, 99–107.

Brackenbury, J. 1997 Caterpillar kinematics. *Nature* **390**, 453. (doi:10.1038/37253)

Candia Carnevali, M. D. 2005 Z-line and supercontraction in the hydraulic muscular system of insect larvae. *J. Exp. Zool.* **203**, 15–29. (doi:10.1002/jez.1402030103)

Dorfmann, A. & Ogden, R. W. 2003 A pseudo-elastic model for loading, partial unloading and reloading of particle-reinforced rubber. *Int. J. Solids Struct.* **40**, 2699–2714. (doi:10.1016/S0020-7683(03)00089-1)

Dorfmann, A. & Ogden, R. W. 2004 A constitutive model for the Mullins effect with permanent set in particle-reinforced rubber. *Int. J. Solids Struct.* **41**, 1855–1878. (doi:10.1016/j.ijsolstr.2003.11.014)

Dorfmann, A. & Ogden, R. W. 2005 Nonlinear electroelasticity. *Acta Mech.* **174**, 167–183. (doi:10.1007/s00707-004-0202-2)

Duch, C., Bayline, R. J. & Levine, R. B. 2000 Postembryonic development of the dorsal longitudinal flight muscle and its innervation in *Manduca sexta*. *J. Comp. Neurol.* **422**, 1–17. (doi:10.1002/(SICI)1096-9861(20000619)422:1<1::AID-CNE1>3.0.CO;2-S)

Dudek, D. M. & Full, R. J. 2006 Passive mechanical properties of legs from running insects. *J. Exp. Zool.* **209**, 1502–1515.

Fukuzawa, A., Shimamura, A., Takemori, S., Kanzawa, N., Yamaguchi, M., Sun, P., Maruyama, K. & Kimura, S. 2001 Invertebrate connection spans as much as 3.5 micrometers in the giant sarcomeres of crayfish claw muscle. *EMBO J.* **20**, 4826–4835. (doi:10.1093/emboj/20.17.4826)

Fung, Y. C. 1980 On pseudo-elasticity of living tissues. In *Mechanics today*, vol. 5 (ed. S. N. Nasser), Pergamon mechanics today series, pp. 49–66. New York, NY: Pergamon Press.

Goldstein, M. A. & Burdette, W. J. 1971 Striated visceral muscle of *Drosophila melanogaster*. *J. Morphol.* **134**, 315–334. (doi:10.1002/jmor.1051340305)

Hardie, J. 1976 The tension/length relationship of an insect (*Calliphora erythrocephala*) supercontracting muscle. *Experientia* **32**, 714–716. (doi:10.1007/BF01919849)

Herrel, A., Meyers, J. J., Timmermans, J. P. & Nishikawa, K. C. 2002 Supercontracting muscle: producing tension over extreme muscle lengths. *J. Exp. Zool.* **205**, 2167–2173.

Hof, A. L. 2003 Muscle mechanics and neuromuscular control. *J. Biomech.* **36**, 1031–1038. (doi:10.1016/S0021-9290(03)00036-8)

Holmes, K. C. & Geeves, M. A. 2000 The structural basis of muscle contraction. *Phil. Trans. R. Soc. B* **355**, 419–431. (doi:10.1098/rstb.2000.0583)

Holzapfel, G. A. 2001 *Nonlinear solid mechanics: a continuum approach for engineering*, 2nd edn. Chichester, UK: Wiley.

Horgan, C. O., Ogden, R. W. & Saccomandi, G. 2004 A theory of stress softening of elastomers based on finite chain extensibility. *Proc. R. Soc. A* **460**, 1737–1754. (doi:10.1098/rspa.2003.1248)

Huxley, A. F. 2000*a* Cross-bridge action: present views, prospects, and unknowns. *J. Biomech.* **33**, 1189–1195. (doi:10.1016/S0021-9290(00)00060-9)

Huxley, A. F. 2000*b* Mechanics and models of the myosin motor. *Phil. Trans. R. Soc. B* **355**, 433–440. (doi:10.1098/rstb.2000.0584)

Jindrich, D. L. & Full, R. J. 2002 Dynamic stabilization of rapid hexapedal locomotion. *J. Exp. Biol.* **205**, 2803–2823.

Karrer, E. 1933 Kinetic theory of the mechanism of muscular contraction. *Protoplasma* **18**, 475–639. (doi:10.1007/BF01611936)

Levine, R. B. & Truman, J. W. 1985 Dendritic reorganization of abdominal motoneurons during metamorphosis of the moth, *Manduca sexta*. *J. Neurosci.* **5**, 2424–2431.

Merodio, J. & Ogden, R. W. 2003 Instabilities and loss of ellipticity in fiber-reinforced compressible non-linearly elastic solids under plane deformation. *Int. J. Solids Struct.* **40**, 4707–4727. (doi:10.1016/S0020-7683(03)00309-3)

Merodio, J. & Ogden, R. W. 2005 Mechanical response of fiber-reinforced incompressible non-linearly elastic solids. *Int. J. Nonlin. Mech.* **40**, 213–227. (doi:10.1016/j.ijnonlinmec.2004.05.003)

Meyer, K. H. 1952 Thermoelastic properties of several biological systems. *Proc. R. Soc. B* **139**, 498–505.

Meyer, K. H., Susich, G. V. & Valkó, E. 1932 The elastic properties of organic high polymers and their kinetic significance. *Kolloid-Zeitschrift* **59**, 208–216. (doi:10.1007/BF01431917)

Ogden, R. W. 1997 *Non-linear elastic deformations*. New York, NY: Dover.

Ogden, R. W. 2001*a* Elements of the theory of finite elasticity. In *Nonlinear elasticity: theory and applications* (eds Y. B. Fu & R. W. Ogden). Cambridge, UK: Cambridge University Press.

Ogden, R. W. 2001*b* Pseudo-elasticity and stress softening. In *Nonlinear elasticity: theory and applications* (eds Y. B. Fu & R. W. Ogden), pp. 491–522. Cambridge, UK: Cambridge University Press.

Ogden, R. W. & Roxburgh, D. G. 1999 A pseudo-elastic model for the Mullins effect in filled rubber. *Proc. R. Soc. A* **455**, 2861–2877. (doi:10.1098/rspa.1999.0431)

Osborne, M. P. 1967 Supercontraction in the muscles of the blowfly larva: an ultrastructural study. *J. Insect. Physiol.* **13**, 1472–1482.

Qiu, G. Y. & Pence, T. J. 1997 Remarks on the behavior of simple directionally reinforced incompressible nonlinearly elastic solids. *J. Elasticity* **49**, 1–30. (doi:10.1023/A:1007410321319)

Rheuben, M. B. & Kammer, A. E. 1980 Comparison of slow larval and fast adult muscle innervated by the same motor neuron. *J. Exp. Biol.* **84**, 103–118.

Rice, M. J. 1970 Supercontracting and non-supercontracting visceral muscles in the tsetse fly, *Glossina austeni*. *J. Insect Physiol.* **16**, 1109–1122. (doi:10.1016/0022-1910(70)90201-5)

Royuela, M., Fraile, B., Arenas, M. I. & Paniagua, R. 2000 Characterization of several invertebrate muscle cell types: a comparison with vertebrate muscles. *Microsc. Res. Tech.* **48**, 107–115. (doi:10.1002/(SICI)1097-0029(20000115)48:2<107::AID-JEMT6>3.0.CO;2-U)

Schwartz, L. M. & Ruff, R. L. 2002 Changes in contractile properties of skeletal muscle during developmentally programmed atrophy and death. *Am. J. Psychol.-Cell Physiol.* **282**, C1270–C1277.

Seipel, J. E., Holmes, P. J. & Full, R. J. 2004 Dynamics and stability of insect locomotion: a hexapedal model for horizontal plane motions. *Biol. Cybern.* **91**, 76–90. (doi:10.1007/s00422-004-0498-y)

Shimada, A., Nyitrai, M., Vetter, I. R., Kuhlmann, D., Bugyi, B., Narumiya, S., Geeves, M. A. & Wittinghofer, A. 2004 The core FH2 domain of diaphanous-related formins is an elongated actin binding protein that inhibits polymerization. *Mol. Cell* **13**, 511–522. (doi:10.1016/S1097-2765(04)00059-0)

Spencer, A. J. M. 1971 Theory of invariants. In *Continuum physics*, vol. 1 (ed. A. C. Eringen), Mathematics, pp. 239–353. New York, NY: Academic Press.

Stevenson, R. D. & Josephson, R. K. 1990 Effects of operating frequency and temperature on mechanical power output from moth flight-muscle. *J. Exp. Biol.* **149**, 61–78.

Treloar, L. R. G. 2005 *The physics of rubber elasticity*. New York, NY: Oxford University Press.

Trimmer, B. A., Takesian, A. E., Sweet, B. M., Rogers, C. B., Hake, D. C. & Rogers, D. J. 2006 Caterpillar locomotion: a new model for soft-bodied climbing and burrowing robots. In *Proc. 7th Int. Symp. on Technology and the Mine Problem*, Monterey, CA: Mine Warfare Association.

Trueman, E. R. 1975 *The locomotion of soft-bodied animals*. London, UK: Edward Arnold.

Wöhlisch, E. 1926 Untersuchungen über elastische thermodynamische, magnetische und elektrische Eigenschaften tierischer Gewebe. *Verhandlungen der physikalisch-medizinischen Gesellschaft in Würzburg* **51**, 53–64.

Woods, W. A., Fusillo, S. J. & Trimmer, B. A. Submitted. Dynamic properties of a locomotory muscle of the tobacco hornworm *Manduca sexta* during strain cycling and simulated natural crawling.

Ziegler, C. 1994 Titin-related proteins in invertebrate muscles. *Comp. Biochem. Phys. A* **109**, 823–833. (doi:10.1016/0300-9629(94)90230-5)